CHEMISTRY OF MATERIALS
Article

Chem. Mater. **2010,** *22,* 5617–5624 5617
DOI:10.1021/cm1019537

Influence of the Annealing Temperature on the Photovoltaic Performance and Film Morphology Applying Novel Thermocleavable Materials

Martin Helgesen,*[,†] Morten Bjerring,[‡] Niels Chr. Nielsen,[‡] and Frederik C. Krebs[†]

[†]*Risø National Laboratory for Sustainable Energy, Technical University of Denmark, Frederiksborgvej 399, DK-4000 Roskilde, Denmark, and* [‡]*Center for Insoluble Protein Structures (inSPIN), Interdisciplinary Nanoscience Center (iNANO) and Department of Chemistry, Aarhus University, DK-8000 Aarhus C, Denmark*

Received July 14, 2010. Revised Manuscript Received August 25, 2010

Di-2-thienyl-2,1,3-benzothiadiazole (DTBT) bearing thermally cleavable ester groups in different positions were prepared and copolymerized with alkylsubstituted cyclopentadithiophene (CPDT). The polymers were found to have band gaps in the range of 1.66−2.03 eV and were explored in polymer photovoltaic devices as mixtures with soluble methanofullerenes. The positioning of the ester groups proved to be very significant despite the identical conjugated backbone of 2-methyl-2-hexyl 5-(4,4-bis(2-ethylhexyl)-4*H*-cyclopenta[1,2-*b*:5,4-*b*′]dithiophen-2-yl)-2-(7-(3-(((2-methylhexan-2-yl)oxy)-carbonyl)thiophen-2-yl)benzo[*c*][1,2,5]thiadiazol-4-yl)thiophene-3-carboxylate (**T1**) and 2-methyl-2-hexyl 2-(4,4-bis(2-ethylhexyl)-4*H*-cyclopenta[1,2-*b*:5,4-*b*′]dithiophen-2-yl)-5-(7-(4-(((2-methylhexan-2-yl)oxy)-carbonyl)thiophen-2-yl)benzo[*c*][1,2,5]thiadiazol-4-yl)thiophene-3-carboxylate (**T2**). Power conversion efficiencies of up to 1.92% were observed for polymers bearing ester groups on the 4-positions of the thienyl groups (**T2**), but shifting them to the 3-positions (**T1**) reduced the efficiency significantly to 0.18%. The thermal behavior of the polymers was studied with thermogravimetric analysis (TGA) that showed a weight loss around 200 °C corresponding to elimination of the ester side chains followed by a second weight loss around 300 °C corresponding to loss of CO_2 via decarboxylation. The temperature of thermocleavage of the active layer films was optimized to 265 °C whereby the **T2**:PCBM solar cells maintained a significant performance giving efficiencies up to 1.49%.

Introduction

From a materials point of view the state-of-the-art in the field of organic photovoltaics is currently represented by bulk heterojunction solar cells based on a polymer/copolymer and a methanofullerene ([60]PCBM and [70]PCBM) where power conversion efficiencies are approaching encouraging 8% for small area devices.[1] The steady increase in performance during the past 10 years reveals a great potential for polymer solar cells as a low-cost renewable energy source,[2−6] but aside from the efficiency, processing and stability are two other important aspects that have to be addressed with equal intensity to fully realize that potential. To combine all three parameters into a useful material and device further research in device science and new materials is needed. A recent approach is to utilize a thermocleavable material which offers significant advantages, both in terms of conjugated polymer synthesis,[7−11] device processing,[3,12,13] and operational stability.[14−17] To overcome the fact that the softness/photochemistry provided by solubilizing chains has been linked to the instability of polymer solar cells,[18−25] the thermocleavable materials exploit a thermally labile bond in the molecule that functions as the linker between

*To whom correspondence should be addressed. E-mail: manp@risoe.dtu.dk.

(1) Chen, H. Y.; Hou, J. H.; Zhang, S. Q.; Liang, Y. Y.; Yang, G. W.; Yang, Y.; Yu, L. P.; Wu, Y.; Li, G. *Nat. Photonics* **2009**, *3*(11), 649–653.
(2) Dennler, G.; Scharber, M. C.; Brabec, C. *J. Adv. Mater.* **2009**, *21* (13), 1323–1338.
(3) Helgesen, M.; Søndergaard, R.; Krebs, F. C. *J. Mater. Chem.* **2010**, *20*(1), 36–60.
(4) Kippelen, B.; Bredas, J. L. *Energy Environ. Sci.* **2009**, *2*(3), 251–261.
(5) Thompson, B. C.; Frechet, J. M. J. *Angew. Chem., Int. Ed.* **2008**, *47* (1), 58–77.
(6) Günes, S.; Neugebauer, H.; Sariciftci, N. S. *Chem. Rev.* **2007**, *107* (4), 1324–1338.
(7) Banishoeib, F.; Adriaensens, P.; Berson, S.; Guillerez, S.; Douheret, O.; Manca, J.; Fourier, S.; Cleij, T. J.; Lutsen, L.; Vanderzande, D. *Sol. Energy Mater. Sol. Cells* **2007**, *91*(11), 1026–1034.
(8) Banishoeib, F.; Henckens, A.; Fourier, S.; Vanhooyland, G.; Breselge, M.; Manca, J.; Cleij, T. J.; Lutsen, L.; Vanderzande, D.; Nguyen, L. H.; Neugebauer, H.; Sariciftci, N. S. *Thin Solid Films* **2008**, *516*(12), 3978–3988.
(9) Girotto, C.; Cheyns, D.; Aernouts, T.; Banishoeib, F.; Lutsen, L.; Cleij, T. J.; Vanderzande, D.; Genoe, J.; Poortman, J.; Heremans, P. *Org. Electron.* **2008**, *9*(5), 740–746.
(10) Palmaerts, A.; Lutsen, L.; Cleij, T. J.; Vanderzande, D.; Pivrikas, A.; Neugebauer, H.; Sariciftci, N. S. *Polymer* **2009**, *50*(21), 5007–5015.
(11) Vandenbergh, J.; Wouters, J.; Adriaensens, P. J.; Mens, R.; Cleij, T. J.; Lutsen, L.; Vanderzande, D. J. M. *Macromolecules* **2009**, *42* (11), 3661–3668.
(12) Hagemann, O.; Bjerring, M.; Nielsen, N. C.; Krebs, F. C. *Sol. Energy Mater. Sol. Cells* **2008**, *92*(11), 1327–1335.
(13) Krebs, F. C.; Norrman, K. *ACS Appl. Mater. Interfaces* **2010**, *2*(3), 877–887.
(14) Bjerring, M.; Nielsen, J. S.; Siu, A.; Nielsen, N. C.; Krebs, F. C. *Sol. Energy Mater. Sol. Cells* **2008**, *92*(7), 772–784.
(15) Gevorgyan, S. A.; Krebs, F. C. *Chem. Mater.* **2008**, *20*(13), 4386–4390.
(16) Krebs, F. C.; Spanggaard, H. *Chem. Mater.* **2005**, *17*(21), 5235–5237.
(17) Krebs, F. C. *Sol. Energy Mater. Sol. Cells* **2008**, *92*(7), 715–726.

Published on Web 09/08/2010

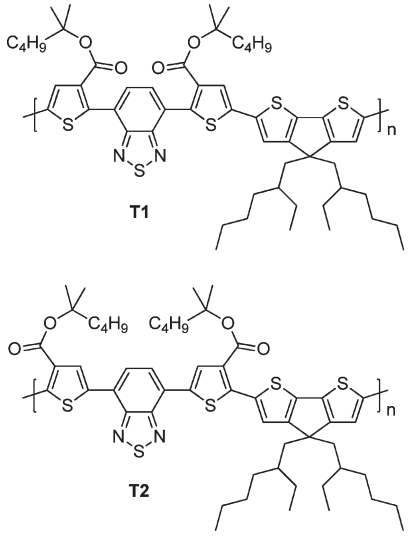

Figure 1. Polymers based on DTBT bearing thermocleavable ester groups and CPDT.

the solubilizing group and the photoactive material. When the polymer is heated this bond breaks whereby the solubilizing group can be removed in a post-processing step forming a harder insoluble material. At this point, thermocleavage of bulk heterojunction polymer:PCBM solar cells has generally lead to a drop in the photovoltaic performance which has been linked to extensive phase segregation of the polymer and PCBM upon annealing.[26] However, there are a few examples where similar or better performance has been obtained after thermocleavage of the film[15,27] and these examples possibly represent cases where the morphology does not change before thermocleavage.

Herein we report our efforts in advancing thermocleavable materials in bulk heterojunction solar cells through the synthesis of two new polymers with reduced band gap. The polymers **T1** and **T2** (Figure 1) are copolymers based on di-2-thienyl-2,1,3-benzothiadiazole (DTBT) and 4,4-bis(2-ethylhexyl)-4*H*-cyclopenta[1,2-*b*:5,4-*b*′]dithiophene (CPDT). For thermocleavability and improved solubility, ester side chains are attached to the thiophene units through a thermally labile ester bond. The ester groups can be removed, at temperatures in the range 200−300 °C, via elimination and decarboxylation in a post-processing step leaving a harder polymer material with high chromophore density. The positioning of the ester groups together with the annealing temperature has a pronounced effect on the photovoltaic performance and film morphology of the polymer:PCBM solar cells which is presented.

Experimental Section

Synthetic procedures for synthesis of monomers and polymers according to Schemes 1 and 2, and their characterization data (incl. ^{1}H and ^{13}C liquid-state -NMR) are described in detail in the Supporting Information together with general experimental details.

Polymer Solar Cell Fabrication and Analysis. Photovoltaic devices were made by spin coating PEDOT:PSS (Aldrich, 1.3 wt % aqueous solution) onto precleaned, patterned indium tin oxide (ITO) substrates (9−15 Ω per square) (LumTec) followed by annealing at 140 °C for 5 min. The active layer was deposited, in a glovebox, by spin coating a blend of the polymer and PCBM dissolved in *o*-dichlorobenzene (40 mg/mL). After a thermal treatment (see Table 2) the counter electrode of aluminum was deposited by vacuum evaporation at $2-3 \times 10^{-6}$ mbar. The active area of the cells was 0.5 cm^2. $I-V$ characteristics were measured under AM1.5G corresponding to 100 mW/cm^2 white light from a multiwavelength high-power LED array using a Keithley 2400 source meter. IPCE spectra were recorded on the same solar test platform[28] with the LED based illumination system.

Results and Discussion

Synthesis. The synthetic steps involved in the preparation of the monomers **7a** and **7b** are outlined in Scheme 1. The esterification of thiophene-3-carboxylic acid (**1**) employs an equivalent amount of 4-dimethylaminopyridine (DMAP) in combination with *N,N*′-diisopropylcarbodiimide (DIPC) giving 2-methyl-2-hexyl thiophene-3-carboxylate (**2**) in high yield. **2** can then be deprotonated in the 2-position using lithium diisopropylamine (LDA) followed by treatment with trimethyltin chloride. This affords the stannylated thiophene **3** which can undergo Stille coupling with 4,7-dibromobenzo[*c*][1,2,5]thiadiazole giving the monomer **6a**. **6a** was finally functionalized by NBS bromination. Activation of **1** in the 5-position is done by dropwise addition of bromine to a solution of **1** in glacial acetic acid which affords 5-bromothiophene-3-carboxylic acid (**4**) in reasonable yield. Using the same procedure as for **2**, esterification of **4** gives the tertiary ester **5** in good yield. Suzuki cross-coupling of **5** with the boronic ester 4,7-bis(4,4,5,5-tetramethyl-1,3,2-dioxaborolan-2-yl)benzo[*c*][1,2,5]thiadiazole affords **6b** which is NBS brominated to give monomer **7b**. Copolymerization of **7a** and **7b** via Stille coupling with the distannylated CPDT unit gives polymer **T1** in 48% yield as a dark red solid (M_w = 57700 g/mol, PDI = 1.9) and **T2** in 89% yield as a dark purple solid (M_w = 41600 g/mol, PDI = 2.7). The solubility of **T1** in organic solvents such as chloroform and toluene is higher than that of **T2** which is probably caused by a more twisted backbone.

Thermal Behavior. The thermal behavior of the thermocleavable polymers was investigated by thermogravimetric

(18) Krebs, F. C.; Norrman, K. *Prog. Photovolt: Res. Appl.* **2007**, *15*(8), 697–712.
(19) Lira-Cantu, M.; Norrman, K.; Andreasen, J. W.; Krebs, F. C. *Chem. Mater.* **2006**, *18*(24), 5684–5690.
(20) Norrman, K.; Krebs, F. C. *Sol. Energy Mater. Sol. Cells* **2006**, *90* (2), 213–227.
(21) Norrman, K.; Larsen, N. B.; Krebs, F. C. *Sol. Energy Mater. Sol. Cells* **2006**, *90*(17), 2793–2814.
(22) Chambon, S.; Rivaton, A.; Gardette, J. L.; Firon, M. *Sol. Energy Mater. Sol. Cells* **2008**, *92*(7), 785–792.
(23) Chambon, S.; Manceau, M.; Firon, M.; Cros, S.; Rivaton, A.; Gardette, J. L. *Polymer* **2008**, *49*(15), 3288–3294.
(24) Manceau, M.; Rivaton, A.; Gardette, J. L. *Macromol. Rapid Commun.* **2008**, *29*(22), 1823–1827.
(25) Manceau, M.; Rivaton, A.; Gardette, J. L.; Guillerez, S.; Lemaitre, N. *Polym. Degrad. Stab.* **2009**, *94*(6), 898–907.
(26) Helgesen, M.; Krebs, F. C. *Macromolecules* **2010**, *43*(3), 1253–1260.
(27) Helgesen, M.; Gevorgyan, S. A.; Krebs, F. C.; Janssen, R. A. J. *Chem. Mater.* **2009**, *21*(19), 4669–4675.
(28) Krebs, F. C.; Sylvester-Hvid, K. O.; Jørgensen, M. Prog. Photovolt: Res. Appl. **2009**, http://dx.doi.org/10.1002/pip.963.

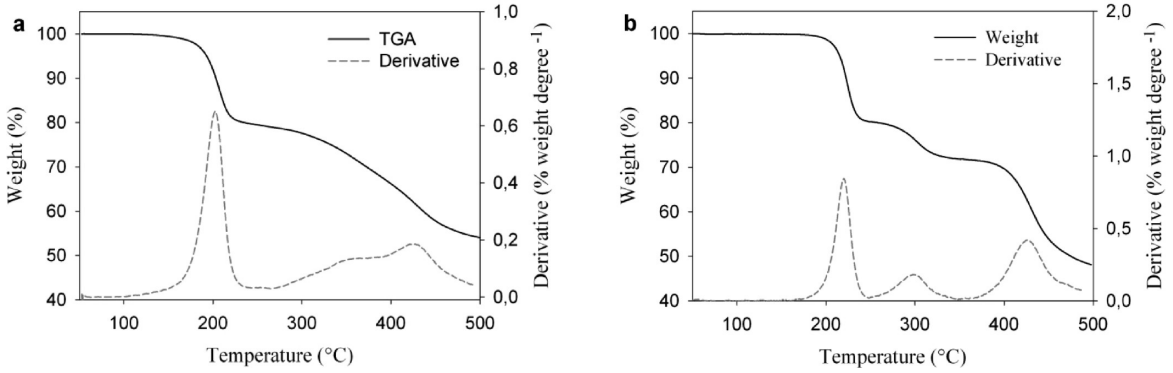

Figure 2. TGA of (a) **T1** and (b) **T2** in the temperature range 50−500 °C. A derivative weight loss curve has been included to tell the point at which weight loss is most apparent.

Scheme 1. Synthetic Steps Involved in the Preparation of the Monomers 7a and 7b

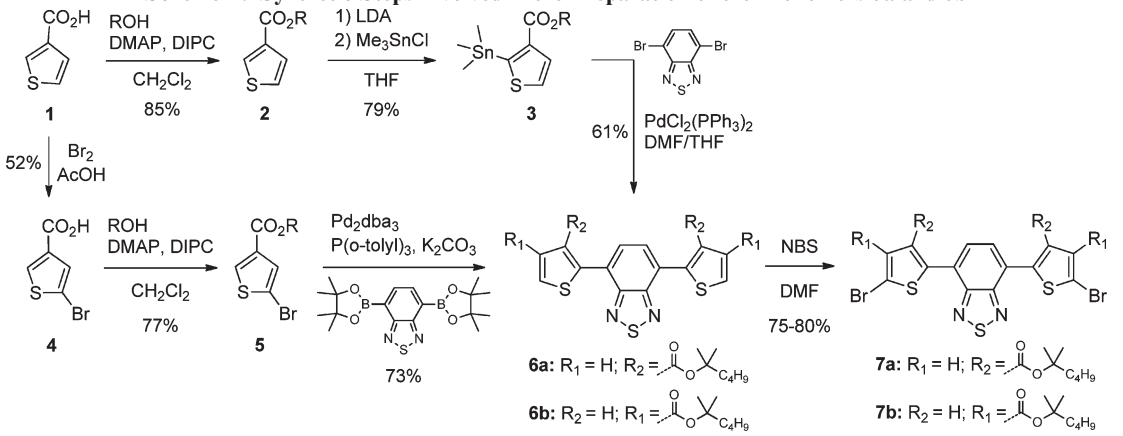

Scheme 2. Synthesis of the Polymers T1 and T2

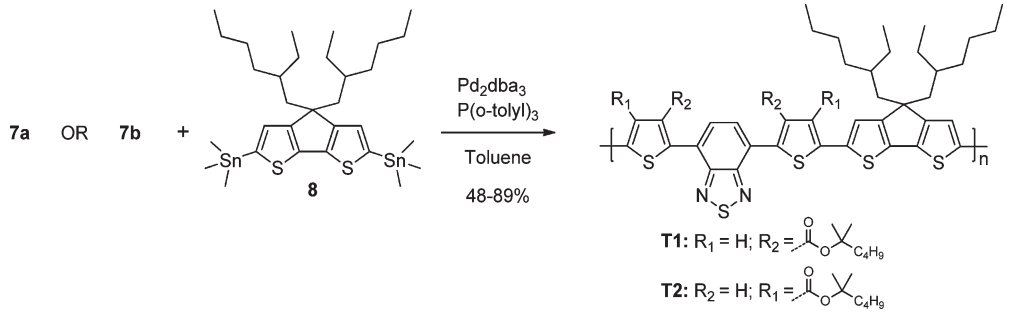

analysis (TGA). The sample holders were carefully weighed, and the samples introduced. TGA was then carried out using heating rate of 10 °C min^{-1}. TGA of **T1** and **T2** in the temperature range 50−500 °C indicates that the ester bond starts to break around 200 °C (Figure 2) as expected from our earlier studies.[27,29] A second loss peak is clearly detected for **T2** at ∼300 °C which corresponds to loss of CO_2.[30] According to Figure 2, the decarboxylation of **T2** starts to happen around 265 °C whereas the exact transition of **T1** is not as clear as for **T2**. At temperatures over 400 °C decomposition of the polymers sets in, and the TGA data of **T1** and **T2** does exhibit the same overall weight loss.

Solid-State NMR. The thermocleavage of the polymers was also followed by solid-state NMR spectroscopy. Here, ^{13}C cross-polarization (CP) magic-angle spinning (MAS) spectra of **T1** and **T2** were acquired before and after heating the materials at 200 and 300 °C for 15 min in a nitrogen atmosphere. Figure 3 shows the ^{13}C CP/MAS spectra of **T1** and **T2** before (a,b), after heating at 200 °C (c,d), and after heating at 300 °C (e,f). It is seen that a large fraction of the aliphatic signals (0−60 ppm) are removed by the heating, indicating that the ester side chains have been cleaved. Also, the signals from the tertiary carbons at the ester side chains at 83 ppm are seen to be totally removed, being consistent with high cleavage efficiency. When heated at 200 °C the ester is converted to a carboxylic acid, for which a characteristic signal at 170 ppm is seen most clearly for **T2** (Figure 3d), and it is evident that this signal

(29) Petersen, M. H.; Gevorgyan, S. A.; Krebs, F. C. *Macromolecules* **2008**, *41*(23), 8986–8994.
(30) Bjerring, M.; Nielsen, J. S.; Nielsen, N. C.; Krebs, F. C. *Macromolecules* **2007**, *40*(16), 6012–6013.

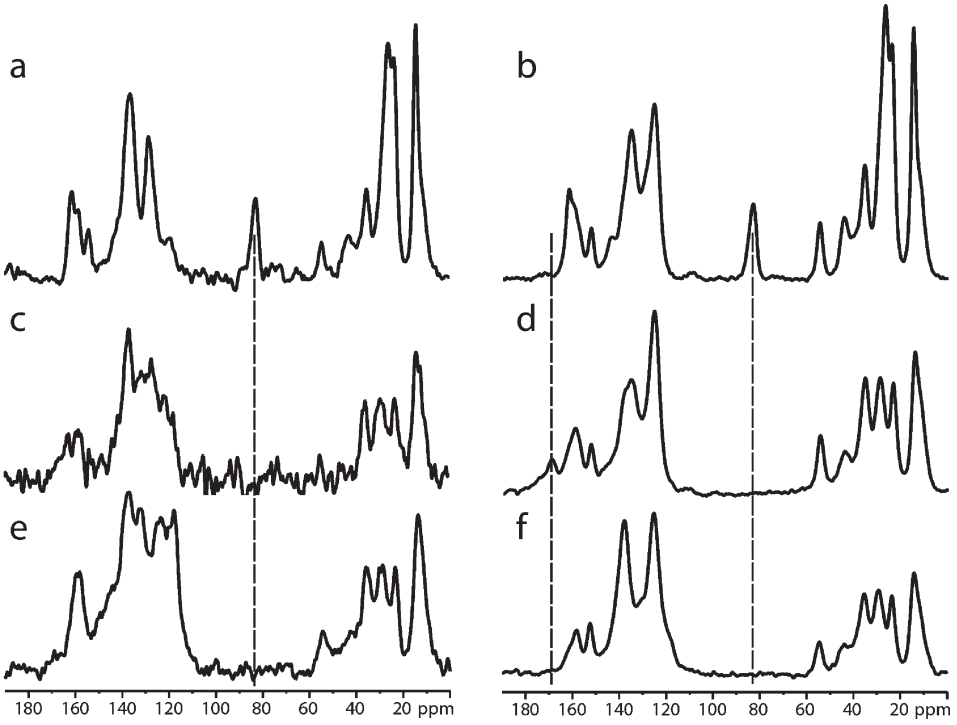

Figure 3. ^{13}C CP/MAS NMR spectra of **T1** (a,c,e) and **T2** (b,d,f) before heating (a,b) and after heating at 200 °C (c,d), 300 °C (e,f) for 15 min. Each spectrum were recorded using 22528 scans in 19 h. The dashed lines at the tertiary carbon and carboxylic acid signals at 83.0 and 169.5 ppm are guides to the eye.

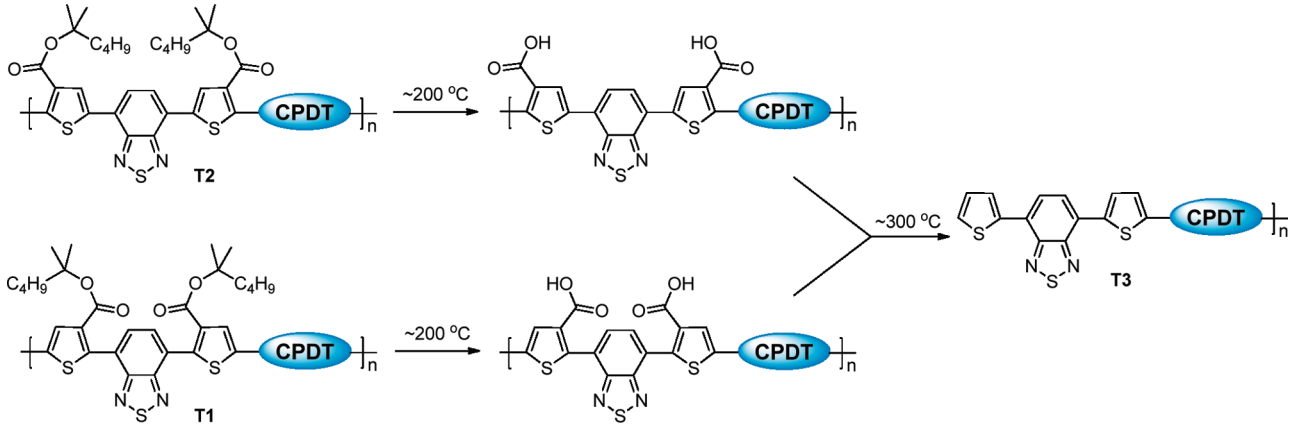

Figure 4. Possible chemical transitions of **T1** and **T2**. The same polymer material is possibly reached after heating at 300 °C.

disappears when the sample is heated at 300 °C (Figure 3f) as a result of the decarboxylation. From this point of view, the same precursor film prepared by standard solution processing of either **T1** or **T2** can thus in principle give access to the same polymer material when heated at 300 °C as shown in Figure 4. The ^{13}C CP/MAS NMR data of **T1** and **T2** do not become identical when heating to 300 °C thus implying that the chemical environment in the solid state differs for the materials obtained after heating. The different chemical environments could arise because of the geometrical constraints imposed by the position of the thermocleavable groups as illustrated in Figure 7 (vide supra).

Optical Properties. The absorption spectra of the polymers in chloroform solution and in thin film are shown in Figures 5 and 6 where a significant effect is observed on the optical properties depending upon where the ester groups are attached on the DTBT unit. In solution the optical band gaps, defined by the onset of absorption, of the polymers range from 1.79 to 2.07 eV (Table 1). The lowest band gap is observed for **T2** suggesting that incorporation of the ester groups on the 4-positions of the thienyl groups introduces minimum steric hindrance to the conjugated backbone thereby improving electron delocalization compared to **T1**. The absorption maxima (λ_{max}) of **T1** is blue-shifted over 100 nm compared to **T2** which also indicate that incorporation of the ester groups on the 3-positions of the thienyl groups will lead to a more twisted conjugated backbone consequently reducing electron delocalization. In thin films, mainly **T2** shows a tendency to π-stack in the solid state where absorption is red-shifted $>$ 50 nm reducing the band gap to 1.66 eV. A minor red shift is observed for **T1** in the solid state giving it a band gap of 2.03 eV. Upon thermocleavage, by annealing at high temperatures for 1 min, the films

maintained the optical quality but showed lower absorption intensity (Figure 6) which might be associated with the change in film thickness and the dielectric constant of the materials. The absorption spectra for **T2** show no significant shifts when the films are annealed but **T1** shows a significant shift toward lower energies after annealing the films at 300 °C. Thermocleavage of the bulky ester groups in the 3-positions of the thienyl groups most likely improve the planarity of the conjugated backbone thereby improving electron delocalization which lowers the band gap. However, the absorption spectra of **T1** and **T2** do not match after thermocleavage at 300 °C (Figure 6) although it should lead to the same material **T3** (Figure 4). This indicates that there are conformational differences in the conjugated backbone of **T1** and **T2** (Figure 7) that get locked through thermocleavage of the ester groups. Consequently, **T1**:PCBM and **T2**:PCBM composites upon heating give **T3**:PCBM composites with the same chemistry, but it is the path to **T3**:PCBM composites that determines the optical properties, photovoltaic performance, and morphology of the final film.

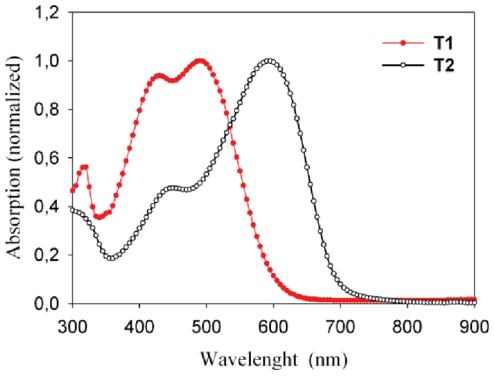

Figure 5. UV−vis absorption spectra of **T1** and **T2** in chloroform solution.

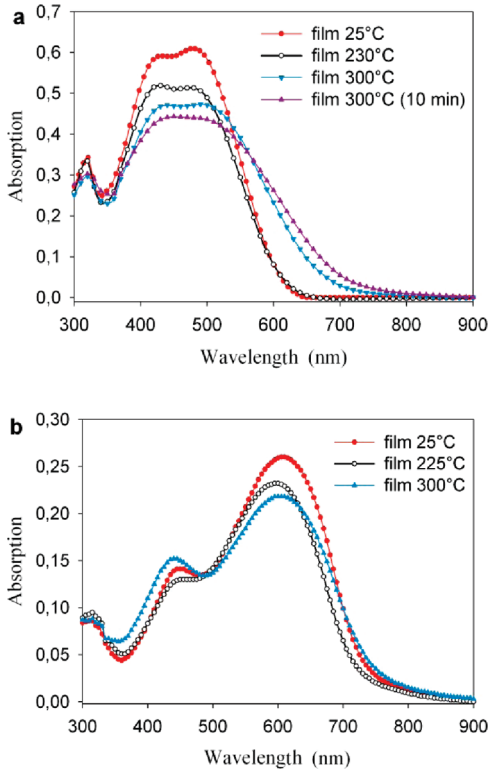

Figure 6. (a) UV−vis absorption spectra of **T1** (native and cleaved) and (b) **T2** (native and cleaved) in thin film before and after thermocleavage for 1 min.

Photovoltaic Performance. Bulk heterojunction solar cells with an active area of 0.5 cm^2 were prepared on an indium tin oxide (ITO) covered glass substrate, using conventional device architecture. A thin layer of poly-(3,4-ethylenedioxythiophene)−poly-(styrenesulfonate) (PEDOT-PSS) was spin coated on top of the ITO coating followed by spin coating of the active layer. The active layer contained a blend of the respective polymer and PCBM. After spin coating of the active layer the devices were either processed directly into a solar cell by evaporation of aluminum as back electrode or subjected to a thermal treatment at the temperature of thermocleavage immediately before evaporation of the back electrode. The most efficient devices comprised a polymer/PCBM ratio of 1:4 spin-coated from *o*-dichlorobenzene with a polymer concentration of 8 mg/mL. The obtained current−voltage curves of the polymer:[60]PCBM solar cells are presented in Figure 8. As discussed above, incorporation of the ester groups on the 3-positions of the thienyl groups in the DTBT unit will introduce significant steric hindrance to the conjugated backbone thereby reducing electron delocalization. The twisted backbone can also weaken intermolecular interactions between the polymer chains in the solid state which could explain the low efficiencies observed for the **T1**:PCBM solar cells (0.15−0.18%). Without thermal treatment of **T1**:PCBM devices a typical V_{oc} of 0.60 V was obtained. Upon heating the device to 225 °C the V_{oc} drops to 0.49 V and is reduced further to 0.42 V when annealing at 265 °C. The current density is enhanced from 1.06 mA/cm^2 to 1.35 mA/cm^2 after thermocleavage at the optimum temperature 265 °C. The effect of thermocleavage is also observed in the incident photon to current efficiency (Figure 9a). For the unannealed **T1**:[60]PCBM solar cells, IPCE is relatively

Table 1. GPC and Spectroscopic Data for Polymers T1 and T2

			solution				film		
polymer	M_w (g/mol)	PDI	$\alpha(\lambda_{max})$ (L/g·cm)	λ_{max} (nm)	λ_{onset} (nm)	E_g (eV)	λ_{max} (nm)	λ_{onset} (nm)	E_g (eV)
T1	57700	1.9	21	490	600	2.07	480 490[a] 456[b]	610 675[a] 715[b]	2.03 1.84[a] 1.73[b]
T2	41600	2.7	27	593	691	1.79	608	746	1.66

[a] Annealed at 300 °C for 1 min. [b] Annealed at 300 °C for 10 min.

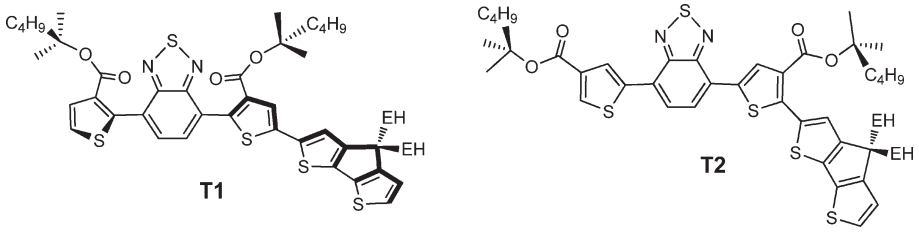

Figure 7. Possible structure of one repeating unit of **T1** (left) and **T2** (right) with minimized energy. MM2 calculation with the software ChemBio3D Ultra (Minimized energy to minimum rms Gradient of 0.100).

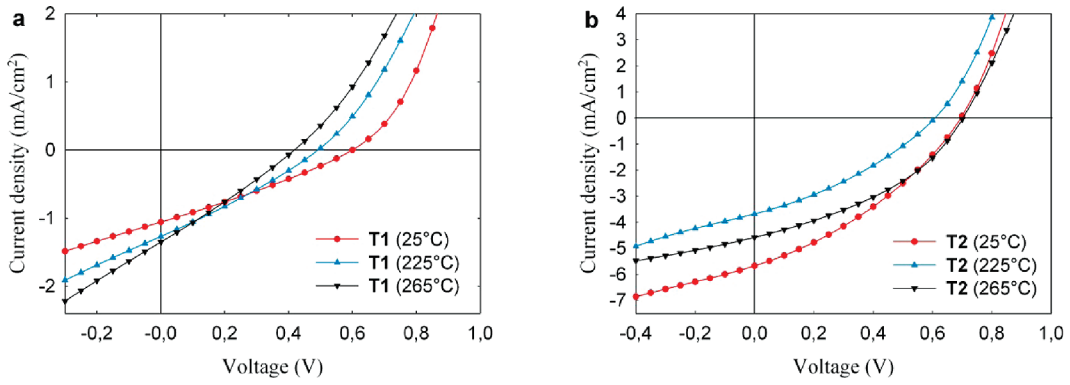

Figure 8. $J-V$ characteristics of (a) **T1**:[60]PCBM solar cells and (b) **T2**:[60]PCBM solar cells measured under 100 mW/cm^2 white light before and after a thermal treatment.

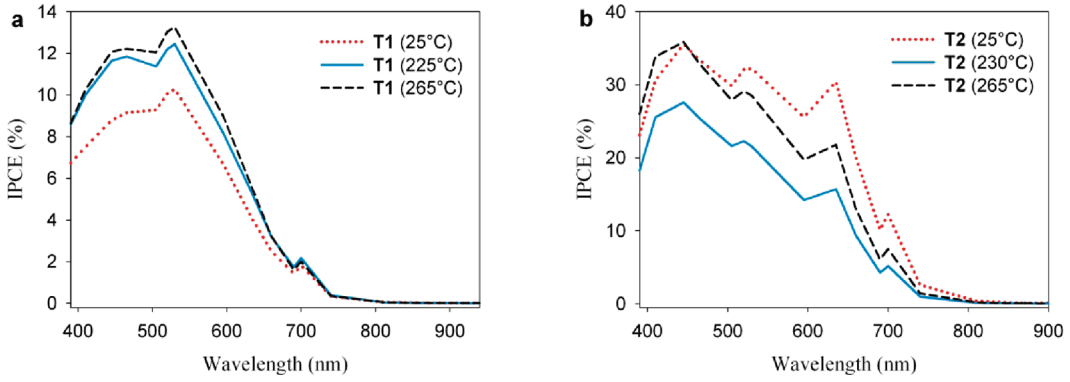

Figure 9. IPCE of (a) **T1**:[60]PCBM solar cells and (b) **T2**:[60]PCBM solar cells before and after a thermal treatment.

low with quantum efficiencies of about 5−10% in the range 390−620 nm but after thermocleavage at 225−265 °C the IPCE increases by up to 4%. The enhanced IPCE after thermocleavage can be explained by partial recovery of the conjugated backbone planarity (i.e., improved charge carrier mobility).

Shifting the ester groups to the 4-position (**T2**) has a major impact on the photovoltaic performance. Without thermal treatment of the **T2**:[60]PCBM solar cells a typical J_{sc} of 5.68 mA/cm^2 was obtained (Table 2). Upon heating the device to 225 °C the J_{sc} drops to 3.68 mA/cm^2 and then increases again to 4.58 mA/cm^2 when annealing at 265 °C. The open-circuit voltage and fill factor experience the same development where you first observe a drop upon annealing at 225 °C followed by an increase when annealing at 265 °C. This results in a nearly retained power conversion efficiency (η = 1.24%) when **T2** is thermocleaved at 265 °C compared to the unannealed device based on the soluble precursor polymer (η = 1.36%). The same effect of annealing is clearly visible in the incident photon to current efficiency (Figure 9b). IPCE lies over 25% (unannealed device) in the wavelength range 400−650 nm reaching a maximum of 36%. After annealing at 225 °C the IPCE drops up to 15% but the initial IPCE is nearly retained when annealing at 265 °C.

Table 2. Photovoltaic Performance of Devices Based on Blends of Polymer and PCBM

polymer	thermal treatment[a] (°C)	V_{oc} (V)	J_{sc} (mA/cm^2)	FF	η (%)
T1		0.60	1.06	0.29	0.18
T1	225	0.49	1.27	0.28	0.17
T1	265	0.42	1.35	0.27	0.15
T2		0.69	5.68	0.35	1.37
T2	225	0.59	3.68	0.33	0.72
T2	265	0.70	4.58	0.38	1.22
T2[b]		0.81	6.79	0.35	1.92
T2[b]	225	0.79	4.55	0.41	1.47
T2[b]	265	0.76	5.61	0.35	1.49

[a] Heated for 20−30 s. [b] Devices prepared with [70]PCBM.

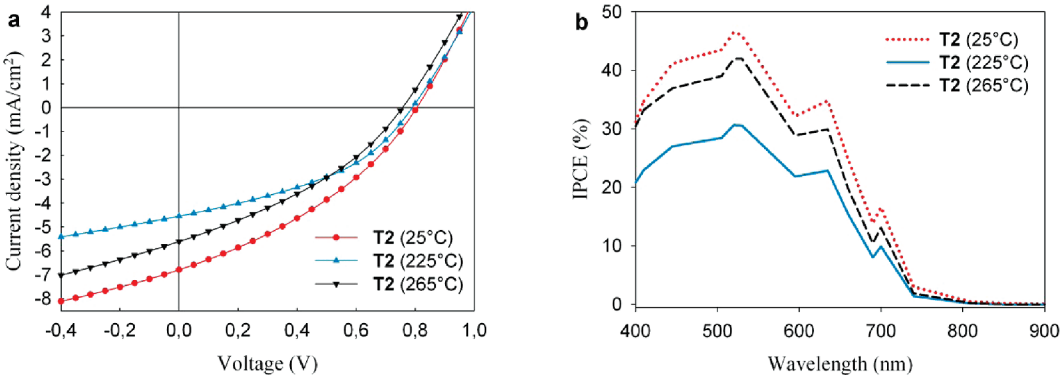

Figure 10. $J-V$ characteristics of (a) **T2**:[70]PCBM solar cells measured under 100 mW/cm^2 white light (b) IPCE of **T2**:[70]PCBM solar cells before and after a thermal treatment.

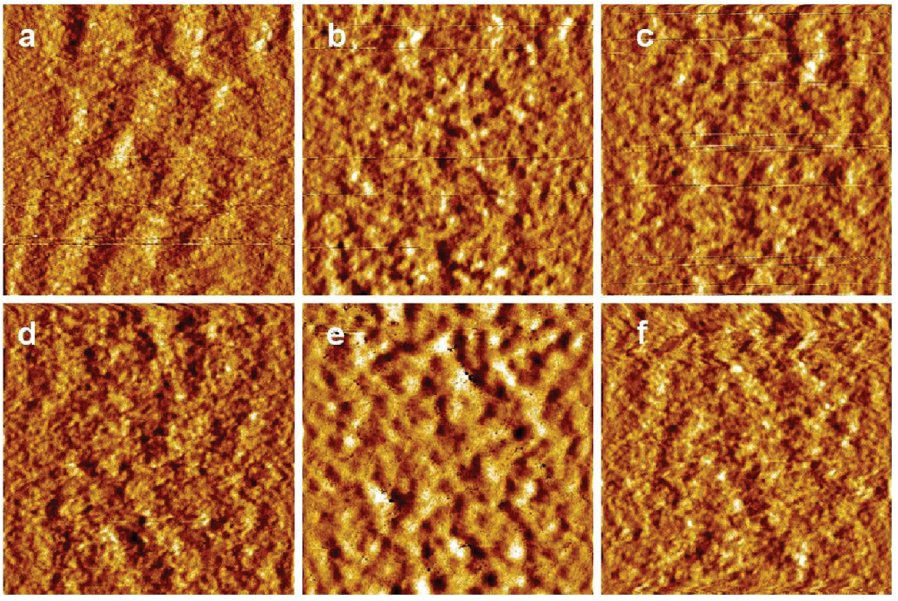

Figure 11. AFM topography images (2 μm × 2 μm) of solar cells based on blends of [60]PCBM and (a) **T1** unannealed, S_q = 0.3 nm, (b) **T1** annealed at 225 °C, S_q = 0.3 nm, (c) **T1** annealed at 265 °C, S_q = 0.3 nm, (d) **T2** unannealed, S_q = 0.3 nm, (e) **T2** annealed at 225 °C, S_q = 0.5 nm, (f) **T2** annealed at 265 °C, S_q = 0.3 nm.

In an attempt to increase the photocurrent, **T2** was also tested in solar cells with [70]PCBM and the obtained $J-V$ curves and IPCE are depicted in Figure 10. [70]PCBM and [60]PCBM has similar electrochemical properties, but [70]PCBM absorbs more light because of its lower symmetry that allow low energy transitions.[31] The incorporation of [70]PCBM improved the performance which is clearly reflected in the IPCE for the unannealed and thermocleaved (265 °C) device which is now found to be higher than 30% in the wavelength range 400−650 nm reaching a maximum of 47% (Figure 10b). A relatively low fill factor limits the power conversion efficiency to 1.49% (thermocleaved at 265 °C) and 1.92% (unannealed). As for **T1**, **T2** can be regarded as thermocleaved to the free carboxylic acid when the device films are annealed at 200−230 °C. However, according to TGA (Figure 2b), the decarboxylation of **T2** start to happen around 265 °C which is also the optimized temperature for thermocleavage of the **T2**:PCBM solar cells. It is likely that thermocleavage under the optimized conditions (265 °C) only leads to partial transformation, where the final film presents chemistry corresponding to both the free carboxylic acid and the decarboxylated material (Figure 4) to varying degrees. Annealing at higher temperatures around 300 °C involved a drastic drop in the V_{oc} and J_{sc} thereby reducing the performance.

Morphology. The performance of bulk heterojunction solar cells based on a mixture of donor and acceptor material is known to be very dependent on the morphology of the active layer.[32−34] Different factors have been shown to have an influence on the morphology including the donor−acceptor ratio, solvent, and the annealing

(31) Wienk, M. M.; Kroon, J. M.; Verhees, W. J. H.; Knol, J.; Hummelen, J. C.; van Hal, P. A.; Janssen, R. A. J. *Angew. Chem., Int. Ed.* **2003**, *42*(29), 3371–3375.

(32) van Duren, J. K. J.; Yang, X. N.; Loos, J.; Bulle-Lieuwma, C. W. T.; Sieval, A. B.; Hummelen, J. C.; Janssen, R. A. J. *Adv. Funct. Mater.* **2004**, *14*(5), 425–434.

(33) Yang, X.; Loos, J. *Macromolecules* **2007**, *40*(5), 1353–1362.

(34) Barrau, S.; Andersson, V.; Zhang, F. L.; Masich, S.; Bijleveld, J.; Andersson, M. R.; Inganas, O. *Macromolecules* **2009**, *42*(13), 4646–4650.

temperature.[26,35−37] Changes in the surface topography of **T1**:PCBM and **T2**:PCBM device films annealed at different temperatures, as measured by atomic force microscopy (AFM), are shown in Figure 11. All films are very smooth with an average surface roughness ranging from 0.3 to 0.5 nm. Comparing the films before and after thermocleavage reveals that only the **T2**:PCBM films shows clear changes in the surface morphology. The domain sizes increase to larger features when the film is annealed at 225 °C (Figure 11e) that indicate extensive phase segregation of the polymer and PCBM which has also been observed in our earlier work.[26] The extensive phase segregation can possibly limit charge carrier generation and transport to the electrodes which might explain the reduced current densities of the **T2**:PCBM devices annealed at 225 °C. The unannealed film and the film annealed at 265 °C (Figure 11d and 11f) reveals a rather uniform phase separation with relatively small domain sizes indicating that thermal cleavage of the tertiary esters at 265 °C takes place before any undesirable change in morphology. Ideally, thermocleavage of the ester groups forms a material with a high glass transition temperature that can limit the possible migration and segregation of the PCBM molecules leading to high thermal stability of the photovoltaic characteristics.[38]

Conclusion

Two new thermocleavable polymers based on di-2-thienyl-2,1,3-benzothiadiazole (DTBT), bearing solubilizing chains on the thienyl groups, and 4,4-bis(2-ethylhexyl)-4*H*-cyclopenta[1,2-*b*:5,4-*b*′]dithiophene (CPDT) have been synthesized. The solubilizing chains on the DTBT unit are thermocleavable alkyl ester groups which allow processing of three chemically different thin films from the same soluble precursor polymer through elimination and decarboxylation. A significant effect is observed on the optical properties and photovoltaic performance depending upon where the ester groups are attached on the DTBT unit. In chloroform solution the polymers had optical band gaps ranging from 1.79 to 2.07 eV that are lowered to 1.66−2.03 eV in thin film (Table 1). The absorption maximum (λ_{max}) of **T1** is blue-shifted over 100 nm compared to that of **T2** which indicates that incorporation of the ester groups on the 3-positions of the thienyl groups will lead to a more twisted conjugated backbone consequently reducing electron delocalization. Furthermore, **T1** shows a significant shift toward lower energies after annealing the films at 300 °C which indicate that thermocleavage of the bulky ester groups in the 3-positions of the thienyl groups most likely improve the planarity of the conjugated backbone.

The best performing polymer in a solar cell was **T2** giving efficiencies up to 1.92% (unannealed) when mixed with [70]PCBM, significantly higher than that of **T1** (η = 0.18%). The greater performance of **T2** suggests that incorporation of the ester groups on the 4-positions of the thienyl groups provide minimum steric hindrance thereby improving electron delocalization and possibly the charge carrier mobility. The temperature of thermocleavage of the active layer films was optimized to 265 °C where the **T2**:PCBM solar cells maintained a significant performance giving efficiencies up to 1.49%.

Acknowledgment. This work was supported by the Danish Strategic Research Council (DSF 2104-05-0052 and 2104-07-0022), the Danish National Research Foundation (through support of inSPIN), and the Danish Biotechnological Instrument Center (DABIC).

Supporting Information Available: General procedures and characterization data including NMR spectra and FTIR spectra of the polymers. Experimental procedures for the synthesis of the monomers and polymers according to Schemes 1 and 2. This material is available free of charge via the Internet at http://pubs.acs.org.

(35) Li, G.; Shrotriya, V.; Yao, Y.; Yang, Y. *J. Appl. Phys.* **2005**, *98*(4), 043704.
(36) Nilsson, S.; Bernasik, A.; Budkowski, A.; Moons, E. *Macromolecules* **2007**, *40*, 8291–8301.
(37) Martens, T.; D'Haen, J.; Munters, T.; Beelen, Z.; Goris, L.; Manca, J.; D'Olieslaeger, M.; Vanderzande, D.; De Schepper, L.; Andriessen, R. *Synth. Met.* **2003**, *138*(1−2), 243–247.
(38) Bertho, S.; Janssen, G.; Cleij, T. J.; Conings, B.; Moons, W.; Gadisa, A.; D'Haen, J.; Goovaerts, E.; Lutsen, L.; Manca, J.; Vanderzande, D. *Sol. Energy Mater. Sol. Cells* **2008**, *92*(7), 753–760.